JOURNAL OF THE MECHANICAL BEHAVIOR OF BIOMEDICAL MATERIALS 38 (2014) 209–218

Available online at www.sciencedirect.com

ScienceDirect

www.elsevier.com/locate/jmbbm

Research Paper

Controlling cell geometry on substrates of variable stiffness can tune the degree of osteogenesis in human mesenchymal stem cells

*Junmin Lee, Amr A. Abdeen, Tiffany H. Huang, Kristopher A. Kilian**

Department of Materials Science and Engineering, Micro and Nanotechnology Laboratory, University of Illinois at Urbana-Champaign, Urbana, IL 61801, USA

ARTICLE INFO

Article history:
Received 19 June 2013
Received in revised form
12 December 2013
Accepted 14 January 2014
Available online 27 January 2014

Keywords:
Substrate stiffness
Microcontact printing
Microenvironment
Polyacrylamide hydrogels
Stem cell differentiation

ABSTRACT

The physical properties of the extracellular matrix (ECM) play an important role in regulating tissue-specific human mesenchymal stem cell (MSC) differentiation. Protein-coated hydrogels with tunable stiffness have been shown to influence lineage specific gene expression in MSCs. In addition, the control of cell shape – either through changing substrate stiffness or restricting spreading with micropatterning – has proved to be important in guiding the differentiation of MSCs. However, few studies have explored the interplay between these physical cues during MSC lineage specification. Here, we demonstrate geometric control of osteogenesis in MSCs cultured on micropatterned polyacrylamide gels. Cells cultured on fibronectin-coated gels express markers associated with osteogenesis in a stiffness dependent fashion with a maximum at ~30 kPa. Controlling the geometry of single cells across the substrate demonstrates elevated osteogenesis when cells are confined to shapes that promote increased cytoskeletal tension. Patterning MSCs across hydrogels of variable stiffness will enable the exploration of the interplay between these physical cues and their relationship with the mechanochemical signals that guide stem cell fate decisions.

1. Introduction

Mesenchymal stem cells (MSCs) isolated from bone marrow, which are a promising source of cells for regenerative medicine and tissue engineering, have the capacity for self-renewal and can differentiate into multiple lineages such as osteogenic, myogenic, adipogenic, chondrogenic, and neurogenic (Crisan et al., 2008; Engler et al., 2006; Pittenger, 1999). The relationship between MSC fate and the structure and properties of the extracellular matrix (ECM) has attracted great attention because the ECM is a key factor in mediating cell apoptosis, proliferation, motility and morphology. Early work by Engler et al. (2006) demonstrated that MSCs could sense the mechanical properties of the ECM to guide differentiation towards neurogenic (<1 kPa), myogenic (~10 kPa), and osteogenic (~30 kPa) lineages. Subsequently, there have been many research efforts to study the mechano-sensitive signal transduction pathways associated with ECM properties in a host of cellular systems (Gilbert et al., 2010; Guvendiren and Burdick, 2012; Keung et al., 2012; Rowlands et al., 2008; Saha et al., 2008; Winer et al., 2009).

*Corresponding author. Tel.: +1 217 244 2142.
E-mail address: kakilian@illinois.edu (K.A. Kilian).

1751-6161/$ - see front matter © 2014 Elsevier Ltd. All rights reserved.
http://dx.doi.org/10.1016/j.jmbbm.2014.01.009

Another important parameter that has been shown to guide MSC differentiation is cell shape which can be controlled by cell seeding density or through micropatterned matrix proteins (Zhang and Kilian, 2013; Gao et al., 2010; McBeath et al., 2004; Théry, 2010; Peng et al., 2012). Mrksich and colleagues used soft lithography to pattern MSCs in an array of different shapes. Cells cultured in geometries with increasing aspect ratio and in ones that present subcellular concave regions beneath the cell led to enhanced non-muscle myosin and rho-associated protein kinase (ROCK) activity which directed initiation of osteogenesis gene expression (Kilian et al., 2010). In addition to these geometric cues, increased cytoskeletal tension through cell spreading has been shown to play a decisive role during MSC differentiation. For example, Chen and colleagues used a micropatterning technique to demonstrate that spread cells are more prone to commit to an osteogenic (McBeath et al., 2004) or smooth muscle myogenic (Gao et al., 2010) lineage compared to adipogenesis or chondrogenesis when exposed to mixed induction cocktails. Both of these cell spreading-related outcomes were shown to be regulated by the small GTPases RhoA (osteogenesis) and Rac (myogenesis), respectively. Other materials-based platforms that influence cell shape, size, and degree of spreading have also been shown to promote the osteogenic differentiation of MSCs (Dalby et al., 2007; Ni et al., 2008; Oh et al., 2009; Yang et al., 1999). Taken together, these studies demonstrate an intimate connection between cell geometry, adhesion architecture and the degree of cytoskeletal tension during MSC osteogenesis. However, the interplay between these physical cues and their respective roles in guiding differentiation remains to be explored.

The development of systems to study the relationships between cell shape and substrate stiffness in the cellular microenvironment is an area of significant interest (Rape et al., 2011; Tang et al., 2012; Tee et al., 2011; Tseng et al., 2011). Recently, we used micropatterned hydrogels to demonstrate how cell spreading and adhesion protein composition can regulate the degree of adipogenesis and neurogenesis on soft substrates (<1 kPa) (Lee et al., 2013). In the present work, we control geometric cues at the single cell level across hydrogels of different stiffness to explore how cell geometry influences osteogenesis on lineage-matched substrates. Using microcontact printing of adhesion proteins on polyacrylamide (PA) gels of variable stiffness, we show that cell shape combined with matrix stiffness can direct the osteogenic differentiation of mesenchymal stem cells. The influence of geometric cues (subcellular curvature and aspect ratio) across the substrate on cell fate decisions is investigated and we show that osteogenesis marker expression can be elevated when cells are confined to shapes that promote increased cytoskeletal tension.

2. Materials and methods

2.1. Materials

Laboratory chemicals and reagents were purchased from Sigma Aldrich unless otherwise noted. Tissue culture plastic ware was purchased from Fisher Scientific. Cell culture media and reagents were purchased from Gibco. Human MSCs and differentiation media were purchased from Lonza. Rabbit anti-Runx2 and anti-Osteopontin were purchased from Abcam. Rabbit anti-Myosin IIb was purchased from Cell signaling Technologies. Tetramethylrhodamine-conjugated anti-rabbit IgG antibody, Alexa488-phalloidin and 4',6-diamidino-2-phenylindole (DAPI) were purchased from Invitrogen. BCIP/NBT solution was purchased from Amresco. Glass coverslips (18-mm circular) for surface preparation were purchased from Fisher Scientific.

2.2. Surface preparation

Polyacrylamide gels were fabricated on a glass cover slip (15 mm) according to established conventional methods (Tse and Engler, 2010). We used the protocol of making hydrogels with varying stiffness by applying a mixture of acrylamide and bis-acrylamide according to the desired stiffness, and for the polymerization, 0.1% ammonium persulfate (APS) and 0.1% of tetramethylethylenediamine (TEMED). 20 μL of the mixture was pipetted onto the hydrophobic treated glass slides, and the amino-silanized coverslips were added with the treated side down (Aratyn-Schaus et al., 2010). After appropriate polymerization time for each stiffness condition (see Fig. S1), the gel-coated cover slips were gently detached. Hydrazine hydrate 55% (Fisher Scientific) was utilized for 1 h to convert amide groups in polyacrylamide to reactive hydrazide groups (Damljanović et al., 2005). Sodium periodate (Sigma-aldrich) was incubated with the glycoproteins to yield free aldehydes. The gels were washed for 1 h in 5% glacial acetic acid (Fluka/Sigma) and for 1 h in distilled water. To create patterned surfaces, polydimethylsiloxane (PDMS, Polysciences, Inc.) stamps were fabricated by polymerization upon a patterned master of photoresist (SU-8, MicroChem) created using UV photolithography through a laser printed mask. 25 μg/mL of fibronectin in PBS was applied for 30 min to the top of patterned or unpatterned PDMS, and then dried under air, and applied to the surface.

2.3. Cell source and culture

Human mesenchymal stem cells (MSCs) from bone marrow were thawed from cryopreservation (10% DMSO) and cultured in Dulbecco's modified Eagle's medium (DMEM) low glucose (1 g/mL) supplemented with 10% fetal bovine serum (MSC approved FBS; Invitrogen), and 1% penicillin/streptomycin (p/s). Media was changed every 4 days and cells were passaged at nearly 80% confluency using 0.25% Trypsin:EDTA (Gibco). Passage 4–7 MSCs were seeded on patterned and non-patterned surfaces at a cell density of ~5000 cells/cm^2.

2.4. Immunocytochemistry

After incubation for 10 days, surfaces were fixed with 4% formaldehyde (Alfa Aesar) for 20 min, and cells were permeablized in 0.1% Triton X-100 in PBS for 30 min and blocked with 1% bovine serum albumin (BSA) for 15 min. Primary antibody labeling was performed in 1% BSA in PBS for 1 h at room temperature (20 °C) with rabbit anti-Runx2, anti-osteopontin or myosin IIb (1:200 dilution). Secondary antibody labeling was performed using the same procedure with tetramethylrhodamine-conjugated anti-rabbit IgG antibody along with Alexa Fluor

488-phalloidin (1:200 dilution) and 4',6-diamidino-2-phenylindole (DAPI, 1:5000 dilution) for 30 min in a humid chamber (37 °C). To stain for alkaline phosphatase, surfaces were rinsed with DI water and incubated for 30 min in BCIP/NBT solution, rinsed well in PBS and imaged in brightfield using a Motic trinocular inverted microscope. Immunofluorescence microscopy was conducted using a Zeiss Axiovert 200 M inverted research-grade microscope (Carl Zeiss, Inc.), and immunofluorescence images were analyzed using ImageJ to measure the fluorescence intensity. The relative intensity of the fluorescence was determined by selecting threshold values and then comparing each data point's raw fluorescence to the established thresholds. For the heatmaps, images were aligned in ImageJ and the intensity across the stack averaged. Color histograms were generated by measuring pixel intensity across the immunofluorescence heatmaps (averaged intensity of stacked images generated in ImageJ) of cells stained for actin or myosin IIb in concave and oval shapes.

2.5. *Atomic force microscopy (AFM)*

The Young's moduli of the surfaces were obtained using AFM contact force measurements on an atomic force microscope (Asylum Research). The AFM tips (Bruker) were calibrated in air and then in phosphate buffered saline (PBS) and all force measurements were performed in PBS. About 10 measurements at different spots were performed for every stiffness condition across 2 samples. The data was fitted into a Hertz model using IGOR PRO software (Wavemetrics). The tip geometry was approximated using a cone architecture to derive the values of Young's modulus.

2.6. *Statistical analysis*

Statistical analysis was performed using one-way ANOVA or Student's *t*-test. Values of $P<0.05$ were considered statistically significant.

3. Results

3.1. *Covalent patterning of matrix protein on polyacrylamide hydrogels of different stiffness*

To study how changing single cell geometry influences MSC differentiation on hydrogels of different stiffness, we developed a procedure to pattern cells on polyacrylamide hydrogels (Fig. 1). We first prepared polyacrylamide (PAAm) hydrogels as previously reported (Tse and Engler, 2010). Since it was shown that hydrogels with around 30 kPa stiffness mimic the rigidity of pre-calcified bone tissue (Engler et al., 2006), we used acrylamide and bis-acrylamide solutions to prepare hydrogels with desired Young's modulus of 10 to 40 kPa (Fig. 2). Next, hydrazine hydrate was applied to the PAAm for converting amide groups in polyacrylamide to reactive hydrazide groups. This treatment allows covalent conjugation of the ECM protein fibronectin (via coupling of formed aldehyde groups after oxidation with sodium periodate) to the surface of the hydrogels. The stiffness of the hydrogels was confirmed by atomic force microscopy (AFM) (Rotsch et al., 1999). We performed 10 different stiffness measurements, and the results showed that measured Young's moduli of hydrogels with desired stiffness of 10, 20, 30, and 40 kPa were 10, 23, 34, and 40, respectively, in close agreement to the targeted range (Fig. 2). To exclude the effects of cell adhesion ligand, we fixed the amount of fibronectin at 25 μg/mL, and thus we could obtain the influence of only varying stiffness. Microcontact printing was used to transfer fibronectin to the hydrazine treated gels with stiffness ranging from 10 to 40 kPa (Fig. 1). First, to fabricate PDMS stamps for microcontact printing, photolithography was employed to obtain patterned structures on the photoresist coated surface of a silicon master. Next, PDMS stamps were prepared by replica molding using liquid PDMS with curing agents over the structured master, and these

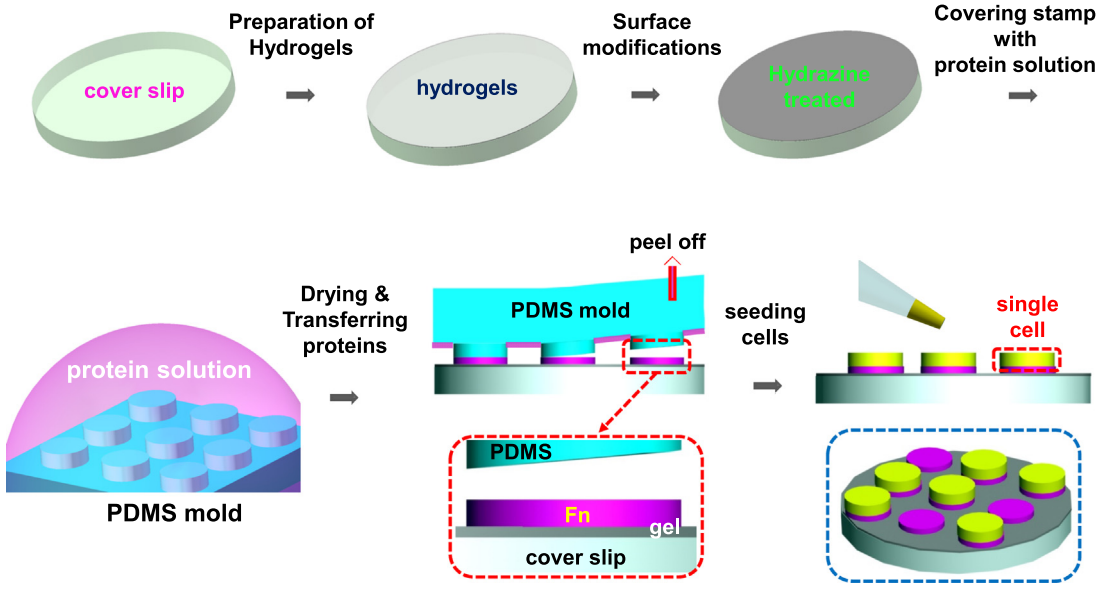

Fig. 1 – Combining geometric cues and substrate stiffness. Schematic illustrating the process used to pattern cells on fibronectin coated polyacrylamide hydrogels.

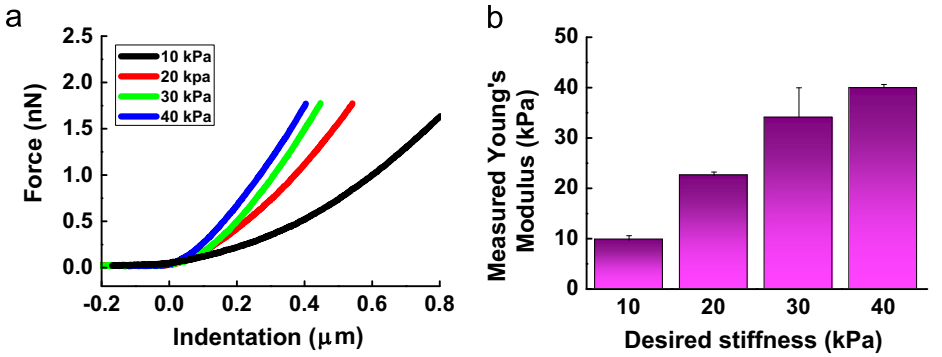

c

Desired Young's Modulus (kPa)	Acrylamide (wt%)	Bis-Acrylamide (wt%)	Measured Young's Modulus (kPa)
10	10	0.100	10 ± 1
20	8	0.264	23 ± 1
30	10	0.250	34 ± 5
40	8	0.480	40 ± 1

Fig. 2 – Characterization of polyacrylamide hydrogels. (a) Force–deflection curves of gels with desired Young's moduli of 10 to 40 kPa (Representative curves). (b) Measured Young's modulus of hydrogels with desired stiffness of 10 to 40 kPa. (c) A table showing the relative concentrations of acrylamide, bis-acrylamide and their desired and measured Young's modulus.

stamps were employed after oxygen plasma treatment to reduce the hydrophobicity on the surface. To confirm the patterning accuracy of deposited protein on the hydrogel substrates, we incorporated fluorescently labeled (Alexa 546) fibrinogen to the oxidized fibronectin solution prior to patterning to confirm protein patterning on the surface and to check pattern fidelity and optimize the process accordingly (Tseng et al., 2011). Immunofluorescence analysis shows that precise patterning of sophisticated features on hydrogels is highly dependent on curing, drying and contact times. For this reason, we optimized the variables from curing time to the method of protein patterning (see Table S1). For example, hydrogel curing time was fixed at ~20–25 min because this led to full polymerization and easy detachment from a hydrophobic glass slide. In addition, drying times for hydrogels and protein solutions on PDMS were empirically determined to be optimal at ~60–90 min and <5 s respectively (see Fig. S1a and 1b). Transferring proteins from the surface of the PDMS stamp to the surface of the hydrogels required complete drying of both surfaces, followed by exposure to trace moisture prior to stamping. Through optimizing all of the variables used in the process, we were able to obtain robust patterning with features resolved down to single microns (Fig. 3a–c, and Fig. S1d).

3.2. *Mesenchymal stem cell culture on hydrogel substrates*

Cells were seeded on fibronectin coated hydrogels and the morphology of the cells was assessed using phase contrast microscopy. Cells on unpatterned gels adhered randomly and displayed a heterogeneous spread phenotype (Fig. 4a). Morphological analysis reveals that the unpatterned cells present a variable spread area dependent on substrate stiffness (10 kPa (~10,000 μm^2) to 40 kPa (~15,000 μm^2), Fig. 4b). On the patterned gels, cells adhered and conformed to the patterned regions after 4 days in culture (Fig. 3d and e). For our initial patterning experiments, we selected geometries that have been shown previously to modulate the degree of cytoskeletal tension while keeping total cell area a constant value (Kilian et al., 2010). The patterned area was chosen to be less than the observed spread area in order to limit proliferation (Zhang and Kilian, 2013) while normalizing the actomyosin contractility state of the single cells across the substrate. Patterned cells adhere to the printed area and show a comparable size to the defined regions (5000 μm^2). In this study, approximately 60–80% of the patterned cells remained viable and restricted to the islands for 10 days in culture. Moreover, we observed that almost all of the cells in patterns on hydrogels did not divide and stayed single cells over the course of the experiment. Since the patterned cells remain in geometric confinement for timescales that have been shown to promote osteogenesis in a substrate-stiffness dependent fashion, we went on to explore the influence of geometry on expression of osteogenesis markers.

3.3. *Osteogenic differentiation of MSCs on micropatterned hydrogel substrates*

Since earlier reports of MSCs undergoing osteogenesis on stiffer matrices used fibronectin as the adhesion protein, we used fibronectin to investigate the degree of osteogenesis on stiffness-tunable hydrogels (~10–40 kPa). Guided by earlier work (Kilian et al., 2010), we hypothesized that elongated shapes and geometries that present features of subcellular

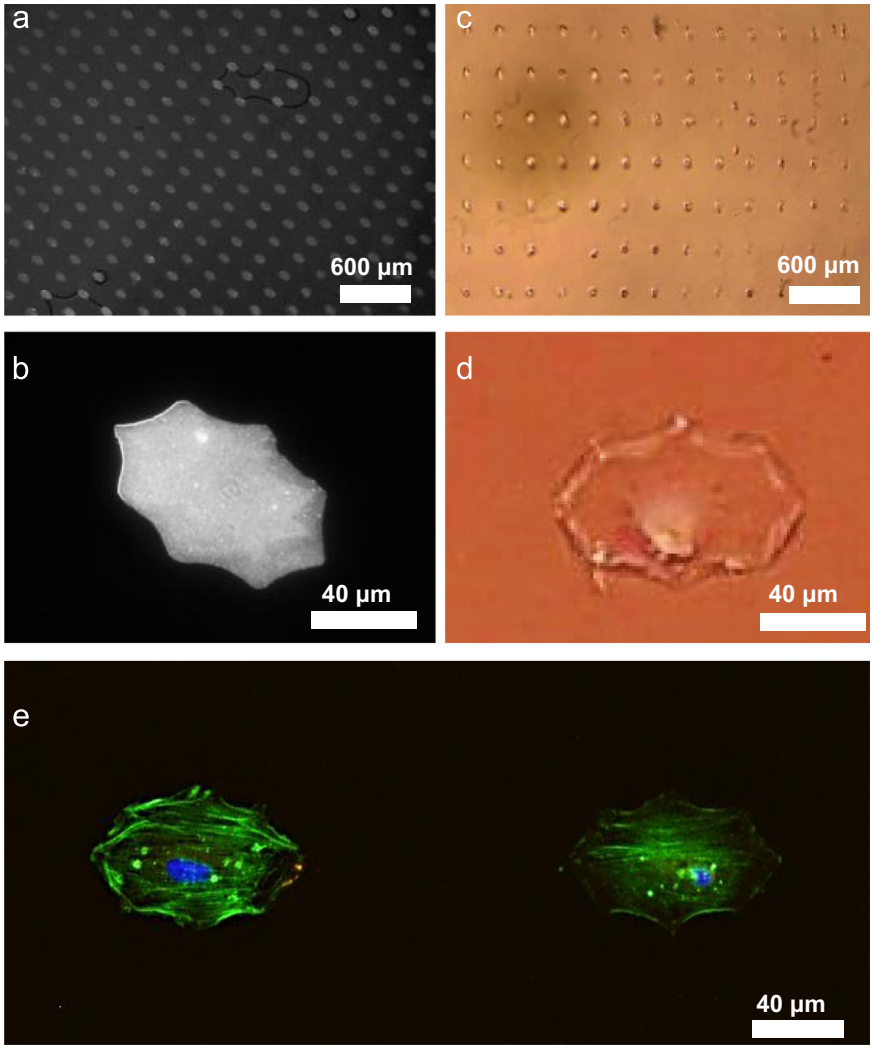

Fig. 3 – Mesenchymal stem cells captured on matrix protein patterned hydrogels. (a) and (b) Representative fluorescence images of patterned adhesion ligands on PA gels with fluorescent fibrinogen (concave shapes). (c) and (d) Representative optical images and (e) immunofluorescence images of cells captured to patterned islands (green-actin; blue-nuclei). (For interpretation of the references to color in this figure legend, the reader is referred to the web version of this article.)

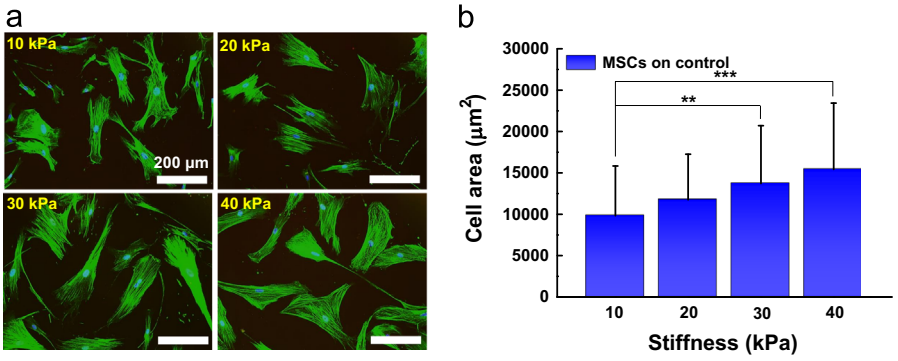

Fig. 4 – Characterizations of mesenchymal stem cells on the gel-protein substrate. (a) Representative images of MSCs on the unpatterned gel–protein substrate. (b) MSC spread area on unpatterned protein-coated hydrogels after 10 days ($P<0.005$, ***$P<0.0005$, *t*-test).**

concavity at the cell perimeter would increase the cytoskeletal tension in MSCs, thus promoting the preference for osteogenesis. To test this hypothesis we designed a range of geometries: a control condition of circular patterns that should yield a low state of cytoskeletal tension in adherent MSCs, shapes of increasing aspect ratio and shapes that

present a combination of subcellular concave features and aspect ratio. MSCs were immunostained for filamentous actin and the non-muscle myosin IIb as a quantitative marker for actomyosin contractility that has previously been shown to mediate osteogenesis in MSCs (Engler et al., 2006; Kilian and Mrksich, 2012; Kilian et al., 2010). Immunofluorescence heatmaps from both stains were generated by averaging the intensity of multiple cells. Heatmaps for MSCs cultured in circular geometries show a uniform and homogenous staining for both actin and myosin IIb (Fig. 5a). In contrast, cells that are cultured in high aspect ratio shapes show increased localization of actin and myosin IIb to regions of high stress along the long edge of the cell. MSCs cultured in geometries that present a combination of aspect ratio and concave features at the perimeter show actin and myosin IIb localizing to regions of cytoskeletal tension that is driven by the cell spanning non-adhesive space fostered by the subcellular concave geometric cues. In addition to differences in average localization of actin and myosin IIb, MSCs cultured in the latter geometries show regions of significantly higher myosin IIb intensity. Quantitation of the myosin IIb intensity across the generated heatmaps reveals marked differences between MSCs cultured in the different shapes (Fig. 5b).

To measure the degree of osteogenesis, we first chose to immunolabel MSCs with the master regulatory transcription factor Runx2, because it is one of the well-known key transcription factors associated with osteoblast differentiation (Komori et al., 1997). Immunofluorescence images were analyzed using ImageJ to measure the fluorescence intensity difference between nuclei and cytoplasm. We observed that

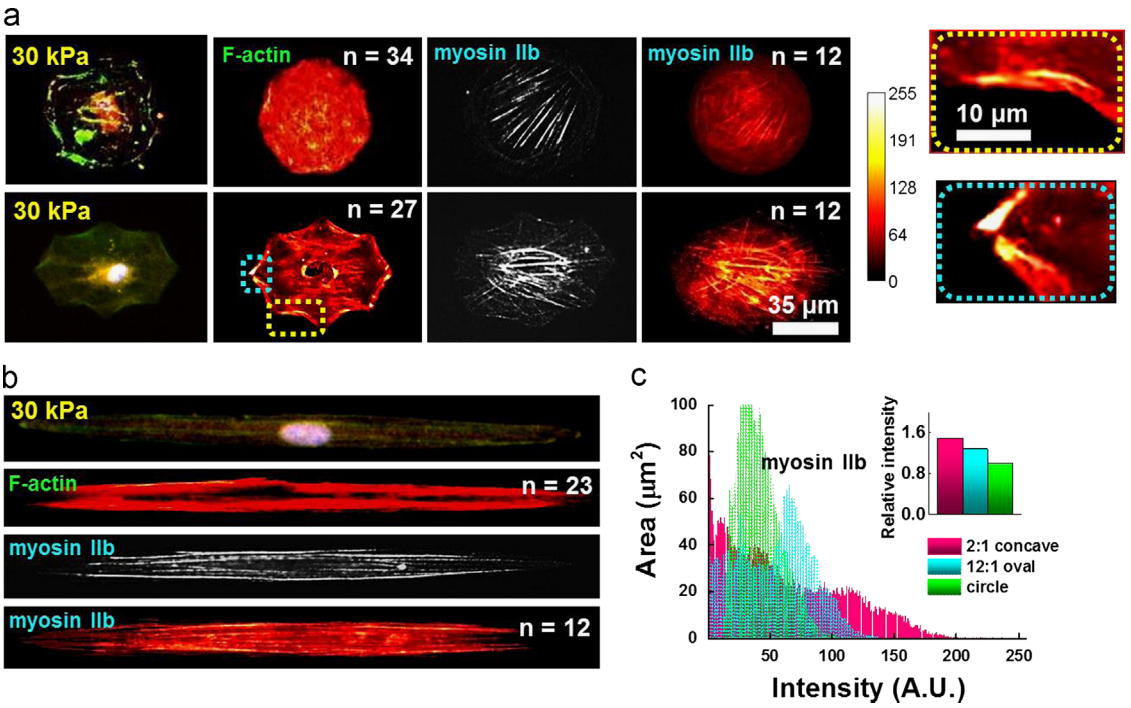

Fig. 5 – Influence of shape on cytoskeleton in mesenchymal stem cells. (a) and (b) Representative immunofluorescence microscopy images and immunofluorescence heatmaps (left to right: F-actin with nuclei, heatmap of F-actin, myosin IIb, and heatmap of myosin IIb) of MSCs cultured in circular, concave, and elongated shapes for 10 days. Expansions in dotted line boxes show regions of high cytoskeletal tension in the heatmaps. (c) Comparison of intensities across the heatmaps of cells stained for myosin IIb. Inset: myosin IIb intensity normalized to the circular geometry for the fluorescence heatmaps of the different patterned cultures (12 cells per pattern).

Fig. 6 – Enhanced osteogenesis marker expression in mesenchymal stem cells patterned in contractile geometries. (a) Relative runx2 marker intensity of cells captured on concave or oval shapes or spread on the fibronectin matrix protein, differentiating to osteogenic lineages (*$P<0.0005$, t-test compared to concave cells on 30 kPa). Runx2 nuclear fluorescence was normalized to cytoplasmic fluorescence. The relative intensity of the fluorescence was determined by comparing each intensity value to the average intensity of spread cells on 10 kPa. (b) Relative osteogenic marker intensity (osteopontin) of cells captured on concave or oval shapes or spread on the fibronectin matrix protein (*$P<0.05$, **$P<0.005$, ***$P<0.0005$, t-test compared to concave cells on 30 kPa). The relative intensity of the fluorescence was determined by comparing each intensity value to the average intensity of spread cells on 10 kPa. (c) Representative immunofluorescence microscopy images (Runx2 and Osteopontin) of MSCs cultured in concave or oval shapes for 10 days. (d) Percentage of cells captured on unpatterned, concave or oval shapes expressing alkaline phosphatase (ALP). (*$P<0.05$, **$P<0.005$, t-test). Representative microscopy images of ALP stained and unstained cells for spread MSCs cultured for 10 days.**

there was no significant difference in Runx 2 expression between spread cells and those confined to circular geometries of comparable area, and both cases expressed Runx2 with a slight stiffness dependence (maximum at ~30 kPa; Fig. S2). Next, we examined the degree of Runx2 expression as well as the early differentiation marker alkaline phosphatase and the late differentiation marker osteopontin for MSCs cultured in our shapes that promote elevated actomyosin contractility. Patterned cells in geometries that increase cytoskeletal tension significantly enhanced the expression

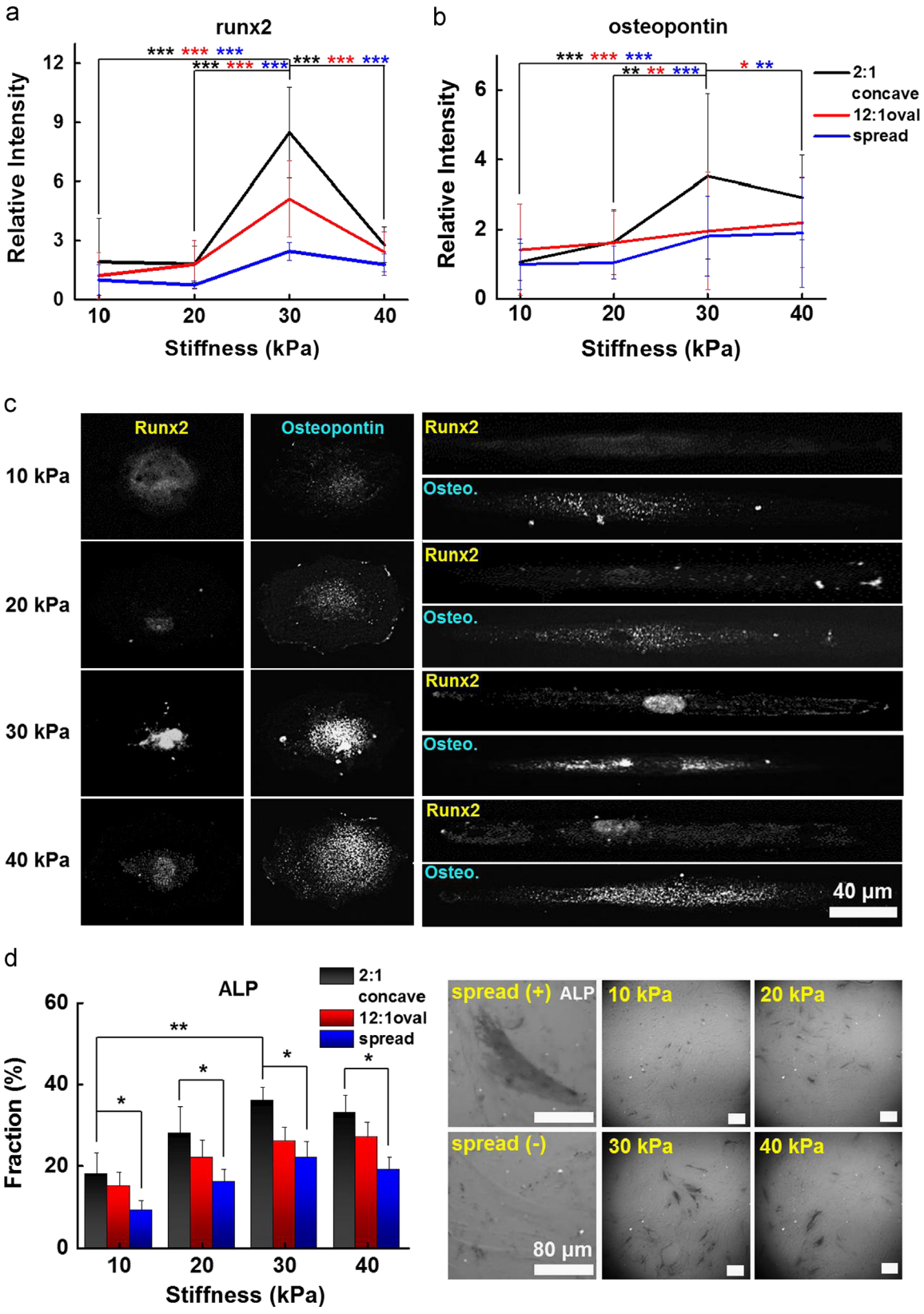

of osteogenesis markers (Fig. 6). MSCs confined to elongated geometries showed approximately 2-fold enhancement in Runx2 expression (at ~30 kPa) compared to unpatterned cells. Interestingly, combining aspect ratio with concave regions at the cell perimeter further enhanced osteogenesis by over 3-fold. We see the similar trends of enhanced osteogenic marker expression for both alkaline phosphatase and osteopontin (Fig. 6b–d) further verifying the Runx2 expression data. From Fig. 6d we see that both increasing stiffness and patterning cells in contractile geometries leads to an increase in differentiation compared to unpatterned populations as determined by alkaline phosphatase staining. These results suggest that normalizing cell shape across substrates with optimal mechanics for the osteogenesis program can be used to tune the desired degree of differentiation.

4. Discussion

Considerable evidence suggests that MSC lineage specification is influenced by substrate stiffness (Engler et al., 2006; Flanagan et al., 2002; Guilak et al., 2009; Higuchi et al., 2013; Khetan et al., 2013; Winer et al., 2009). The tendency for cells to pull against and deform the matrix through specific integrin-mediated interactions with matrix proteins plays a significant role in guiding downstream signal transduction that regulates gene expression (Aratyn-Schaus et al., 2010; Damljanović et al., 2005; Frith et al., 2012; Kurpinski et al., 2006; McGarry et al., 2009). Actin filaments anchored at focal adhesions are important structures for force transmission in order for cells to feel the compliance of their substrate. (Kilian et al., 2010; Trappmann et al., 2012; Yim et al., 2010). In this way, stiff matrices give rise to increased cell spreading which has been shown to promote osteogenesis through enhanced actomyosin contractility.

MSCs cultured on hydrogels modified with matrix protein display a range of morphologies and heterogeneous differentiation outcomes in response to substrate rigidity. Recent work by Burdick and colleagues has demonstrated that the heterogeneity of MSC differentiation depends on the time in culture prior to matrix stiffening (Guvendiren and Burdick, 2012). Furthermore, we recently found that restricting cell spreading using micropatterned substrates can decrease heterogeneity associated with the expression of osteogenic markers in MSC cultures (Zhang and Kilian, 2013). We hypothesized that micropatterning cells across hydrogel substrates with mechanical properties of pre-calcified bone would influence the degree of osteogenesis by normalizing each cell to experience approximately the same mechanical microenvironment. Evidence to support this comes from recent work that demonstrated how geometric features that promote actomyosin contractility have been shown to enhance osteogenesis in patterned MSCs that are exposed to lineage-guiding media supplements (Kilian et al., 2010; Peng et al., 2012). To test this hypothesis, we first patterned MSCs in a circular shape that does not contain geometric cues that promote cytoskeletal tension. MSCs cultured in this shape displayed a disordered cytoskeleton and did not increase the expression of nuclear Runx2 when compared to the population of unpatterned cells. To investigate how shape may enhance osteogenesis on hydrogels, we explored geometric features that are known to increase actomyosin contractility: a 12:1 aspect ratio oval and a shape with moderate aspect ratio and regions of subcellular concavity. We see a stiffness dependence in the expression of osteogenic markers with a maximum at ~30 kPa, in agreement with previous reports (Engler et al., 2006). MSCs that are cultured in geometries that promote increased cytoskeletal tension show a further enhancement – particularly at the osteogenic stiffness of ~30 kPa – of 2-fold (elongated oval shape) and >3-fold (concave shape). Since unpatterned cells display a range of morphologies, the average expression measured from this heterogeneous population is variable. Using micropatterning, the cytoskeletal tension of the entire population of cells can be normalized, thus influencing the final degree of osteogenesis.

5. Conclusions

Signaling in mesenchymal stem cells is influenced by the physical aspects of the microenvironment including mechanical properties, geometry and topography. In this work, we show how microengineered hydrogels can be used to combine several of these physical cues to explore MSC differentiation. Cells cultured on protein coated gels show a stiffness dependence in the expression of markers associated with osteogenesis. Patterning single MSCs in isotropic circles show no appreciable difference in osteogenic marker expression compared to the unpatterned cells. In contrast, MSCs cultured in shapes that present geometric cues to enhance cytoskeletal tension show a significant increase. This result demonstrates how osteogenesis in adherent MSCs can be controlled by both cell geometry and the mechanics of the substrate. We expect this platform will be broadly applicable across other differentiation events and other stem cell systems that are influenced by the physical microenvironment. This strategy is expected to prove particularly useful in stem cell mechanobiology investigations where control of multiple extracellular parameters will be advantageous to study and direct lineage specification and commitment.

Acknowledgments

This work was supported by start-up funding from the University of Illinois at Urbana-Champaign, College of Engineering, Department of Materials Science and Engineering. We gratefully acknowledge the assistance of Alex Cargill in CAD art design for generating the photolithography masks.

Appendix A. Supplementary material

Supplementary data associated with this article can be found in the online version at http://dx.doi.org/10.1016/j.jmbbm.2014.01.009.

REFERENCES

Aratyn-Schaus, Y., Oakes, P.W., Stricker, J., Winter, S.P., Gardel, M.L., 2010. Preparation of complaint matrices for quantifying cellular contraction. J. Vis. Exp, 1–6.

Crisan, M., Yap, S., Casteilla, L., Chen, C.-W., Corselli, M., Park, T. S., Andriolo, G., Sun, B., Zheng, B., Zhang, L., Norotte, C., Teng, P.-N., Traas, J., Schugar, R., Deasy, B.M., Badylak, S., Buhring, H.-J., Giacobino, J.-P., Lazzari, L., Huard, J., Péault, B., 2008. A perivascular origin for mesenchymal stem cells in multiple human organs. Cell Stem Cell 3, 301–313.

Dalby, M.J., Gadegaard, N., Tare, R., Andar, A., Riehle, M.O., Herzyk, P., Wilkinson, C.D.W., Oreffo, R.O.C., 2007. The control of human mesenchymal cell differentiation using nanoscale symmetry and disorder. Nat. Mater. 6, 997–1003.

Damljanović, V., Lagerholm, B.C., Jacobson, K., 2005. Bulk and micropatterned conjugation of extracellular matrix proteins to characterized polyacrylamide substrates for cell mechanotransduction assays. Biotechniques 39, 847–851.

Engler, A.J., Sen, S., Sweeney, H.L., Discher, D.E., 2006. Matrix elasticity directs stem cell lineage specification. Cell 126, 677–689.

Flanagan, L.A., Ju, Y., Marg, B., Osterfield, M., Paul, A., 2002. Neuroreport 13, 2411–2415.

Frith, J.E., Mills, R.J., Hudson, J.E., Cooper-White, J.J., 2012. Tailored integrin-extracellular matrix interactions to direct human mesenchymal stem cell differentiation. Stem Cells Dev. 21, 2442–2456.

Gao, L., McBeath, R., Chen, C.S., 2010. Stem cell shape regulates a chondrogenic versus myogenic fate through Rac1 and N-cadherin. Stem Cells 28, 564–572.

Gilbert, P.M., Havenstrite, K.L., Magnusson, K.E.G., Sacco, a, Leonardi, N. a, Kraft, P., Nguyen, N.K., Thrun, S., Lutolf, M.P., Blau, H.M., 2010. Substrate elasticity regulates skeletal muscle stem cell self-renewal in culture. Science 80 (329), 1078–1081.

Guilak, F., Cohen, D.M., Estes, B.T., Gimble, J.M., Liedtke, W., Chen, C.S., 2009. Control of stem cell fate by physical interactions with the extracellular matrix. Cell Stem Cell 5, 17–26.

Guvendiren, M., Burdick, J. a, 2012. Stiffening hydrogels to probe short- and long-term cellular responses to dynamic mechanics. Nat. Commun 3, 792.

Higuchi, A., Ling, Q., Chang, Y., Hsu, S., Umezawa, A., 2013. Physical cues of biomaterials guide stem cell differentiation fate. Chem. Rev 113, 3297–3328.

Keung, A.J., Asuri, P., Kumar, S., Schaffer, D.V, 2012. Soft microenvironments promote the early neurogenic differentiation but not self-renewal of human pluripotent stem cells. Integr. Biol. 4, 1049–1058.

Khetan, S., Guvendiren, M., Legant, W.R., Cohen, D.M., Chen, C.S., Burdick, J. a, 2013. Degradation-mediated cellular traction directs stem cell fate in covalently crosslinked three-dimensional hydrogels. Nat. Mater. 12, 1–8.

Kilian, K. a, Bugarija, B., Lahn, B.T., Mrksich, M., 2010. Geometric cues for directing the differentiation of mesenchymal stem cells. Proc. Nat. Acad. Sci. U.S.A. 107, 4872–4877.

Kilian, K.a, Mrksich, M., 2012. Directing stem cell fate by controlling the affinity and density of ligand-receptor interactions at the biomaterials interface. Angew. Chem. Int. Ed. Engl 51, 4891–4895.

Komori, T., Yagi, H., Nomura, S., Yamaguchi, a, Sasaki, K., Deguchi, K., Shimizu, Y., Bronson, R.T., Gao, Y.H., Inada, M., Sato, M., Okamoto, R., Kitamura, Y., Yoshiki, S., Kishimoto, T, 1997. Targeted disruption of Cbfa1 results in a complete lack of bone formation owing to maturational arrest of osteoblasts. Cell 89, 755–764.

Kurpinski, K., Chu, J., Hashi, C., Li, S., 2006. Anisotropic mechanosensing by mesenchymal stem cells. Proc. Nat. Acad. Sci. U.S.A. 103, 16095–16100.

Lee, J., Abdeen, A. a, Zhang, D., Kilian, K. a, 2013. Directing stem cell fate on hydrogel substrates by controlling cell geometry, matrix mechanics and adhesion ligand composition. Biomaterials 34, 8140–8148.

McBeath, R., Pirone, D.M., Nelson, C.M., Bhadriraju, K., Chen, C.S., 2004. Cell shape, cytoskeletal tension, and RhoA regulate stem cell lineage commitment. Dev. Cell 6, 483–495.

McGarry, J.P., Fu, J., Yang, M.T., Chen, C.S., McMeeking, R.M., Evans, a G., Deshpande, V.S., 2009. Simulation of the contractile response of cells on an array of micro-posts. Philos. Trans. R. Soc. London, Ser. A 367, 3477–3497.

Ni, X.F., Crozatier, C., Sensebé, L., Langonne, a., Wang, L., Fan, Y., He, P.G., Chen, Y., 2008. On-chip differentiation of human mesenchymal stem cells into adipocytes. Microelectron. Eng. 85, 1330–1333.

Oh, S., Brammer, K.S., Li, Y.S.J., Teng, D., Engler, A.J., Chien, S., Jin, S., 2009. Stem cell fate dictated solely by altered nanotube dimension. Proc. Nat. Acad. Sci. U.S.A. 106, 2130–2135.

Peng, R., Yao, X., Cao, B., Tang, J., Ding, J., 2012. The effect of culture conditions on the adipogenic and osteogenic inductions of mesenchymal stem cells on micropatterned surfaces. Biomaterials 33, 6008–6019.

Pittenger, M.F., 1999. Multilineage potential of adult human mesenchymal stem cells. Science 80 (284), 143–147.

Rape, A.D., Guo, W.-H., Wang, Y.-L., 2011. The regulation of traction force in relation to cell shape and focal adhesions. Biomaterials 32, 2043–2051.

Rotsch, C., Jacobson, K., Radmacher, M., 1999. Dimensional and mechanical dynamics of active and stable edges in motile fibroblasts investigated by using atomic force microscopy. Proc. Nat. Acad. Sci. U.S.A. 96, 921–926.

Rowlands, A.S., George, P.a, Cooper-White, J.J., 2008. Directing osteogenic and myogenic differentiation of MSCs: interplay of stiffness and adhesive ligand presentation. Am. J. Physiol. Cell Physiol 295, C1037–C1044.

Saha, K., Keung, A.J., Irwin, E.F., Li, Y., Little, L., Schaffer, D.V, Healy, K.E., 2008. Substrate modulus directs neural stem cell behavior. Biophys. J. 95, 4426–4438.

Tang, X., Yakut Ali, M., Saif, M.T.A., 2012. A novel technique for micro-patterning proteins and cells on polyacrylamide gels. Soft Matter 8, 7197–7206.

Tee, S.-Y., Fu, J., Chen, C.S., Janmey, P. a, 2011. Cell shape and substrate rigidity both regulate cell stiffness. Biophys. J. 100, L25–L27.

Théry, M., 2010. Micropatterning as a tool to decipher cell morphogenesis and functions. J. Cell Sci 123, 4201–4213.

Trappmann, B., Gautrot, J.E., Connelly, J.T., Strange, D.G.T., Li, Y., Oyen, M.L., Cohen Stuart, M. a, Boehm, H., Li, B., Vogel, V., Spatz, J.P., Watt, F.M., Huck, W.T.S., 2012. Extracellular-matrix tethering regulates stem-cell fate. Nat. Mater. 11, 642–649.

Tse, J.R., Engler, A.J., 2010. Preparation of hydrogel substrates with tunable mechanical properties. Curr. Protoc. Cell Biol, 16 (Chapter 10, Unit 10.).

Tseng, Q., Wang, I., Duchemin-Pelletier, E., Azioune, A., Carpi, N., Gao, J., Filhol, O., Piel, M., Théry, M., Balland, M., 2011. A new micropatterning method of soft substrates reveals that different tumorigenic signals can promote or reduce cell contraction levels. Lab Chip 11, 2231–2240.

Winer, J.P., Janmey, P. a, McCormick, M.E., Funaki, M., 2009. Bone marrow-derived human mesenchymal stem cells become quiescent on soft substrates but remain responsive to chemical or mechanical stimuli. Tissue Eng. Part A 15, 147–154.

Yang, Relan, N.K., Przywara, D.A., Schuger, L., 1999. Embryonic mesenchymal cells share the potential for smooth muscle differentiation: myogenesis is controlled by the cell's shape 3033, 3027–3033.

Yim, E.K., Darling, E.M., Kulangara, K., Guilak, F., Leong, K.W., 2010. Nanotopography-induced changes in focal adhesions, cytoskeletal organization, and mechanical properties of human mesenchymal stem cells. Biomaterials 31, 1299–1306.

Zhang, D., Kilian, K.a, 2013. The effect of mesenchymal stem cell shape on the maintenance of multipotency. Biomaterials 34, 3962–3969.